

1 **Supporting Information**

2

3 **Synergy of non-lithium cation doping and lithium concentration**
4 **affecting lithium ion transport in solid electrolyte**

5 Shihao Feng^a, Zhixing Wang^{a,b,c}, Huajun Guo^{a,b,c}, Xinhai Li^{a,b,c}, Guochun

6 Yan^{a,c}, Qihou Li,^{a,*} Jiexi Wang^{a,b,c,*}

7

8 ^a School of Metallurgy and Environment, Central South University, 410083

9 Changsha, P. R. China

10 ^b Engineering Research Center of the Ministry of Education for Advanced

11 Battery Materials, Central South University, Changsha, 410083, P. R. China

12 ^c Hunan Provincial Key Laboratory of Nonferrous Value-Added Metallurgy,

13 Central South University, Changsha, 410083, P. R. China

14

15 * Corresponding author, email address: liqihou@csu.edu.cn (Q.Li);

16 wangjiexikeen@csu.edu.cn (J.Wang)

17

1 **Table S1.** Calculated lattice parameters of $\text{Li}_{16-2x}\text{Zn}_x\text{Ge}_4\text{O}_{16}$ and Li_{16-}
 2 $_{2x}\text{Mg}_x\text{Ge}_4\text{O}_{16}$ from DFT.

Composition	cell	a (Å)	b (Å)	c (Å)	α (°)	β (°)	γ (°)	Unit cell Volume (Å ³)
$\text{Li}_{12}\text{Mg}_2\text{Ge}_4\text{O}_{16}$	supercell	10.57	12.71	10.99	90.00	90.51	89.29	1477.03
$\text{Li}_{14}\text{MgGe}_4\text{O}_{16}$	supercell	10.50	12.58	10.97	90.02	90.12	90.68	1448.86
$\text{Li}_{15}\text{Mg}_{0.5}\text{Ge}_4\text{O}_{16}$	supercell	10.94	12.60	10.43	89.90	89.90	90.17	1437.76
$\text{Li}_{15.5}\text{Mg}_{0.25}\text{Ge}_4\text{O}_{16}$	supercell	10.93	12.58	10.45	89.96	89.95	90.09	1435.30
$\text{Li}_{12}\text{Zn}_2\text{Ge}_4\text{O}_{16}$	supercell	10.58	12.62	10.99	90.04	91.08	89.85	1467.29
$\text{Li}_{14}\text{ZnGe}_4\text{O}_{16}$	supercell	10.50	12.60	10.95	90.01	89.94	90.52	1449.85
$\text{Li}_{15}\text{Zn}_{0.5}\text{Ge}_4\text{O}_{16}$	supercell	10.91	12.56	10.43	89.95	90.27	89.93	1429.10

3

4

5 **Table S2.** The phase stability and diffusional properties of $\text{Li}_{16-2x}\text{Zn}_x\text{Ge}_4\text{O}_{16}$
 6 and $\text{Li}_{16-2x}\text{Mg}_x\text{Ge}_4\text{O}_{16}$.

Composition	E_{hull} (meV/atom)	$\sigma_{300\text{K}}$ (mS/cm)	E_a (eV)
$\text{Li}_{12}\text{Zn}_2\text{Ge}_4\text{O}_{16}$	15	0.16	0.34
$\text{Li}_{14}\text{ZnGe}_4\text{O}_{16}$	23	2.50	0.27
$\text{Li}_{15}\text{Zn}_{0.5}\text{Ge}_4\text{O}_{16}$	27	1.16	0.30
$\text{Li}_{12}\text{Mg}_2\text{Ge}_4\text{O}_{16}$	17	0.01	0.42
$\text{Li}_{14}\text{MgGe}_4\text{O}_{16}$	24	0.15	0.35
$\text{Li}_{15}\text{Mg}_{0.5}\text{Ge}_4\text{O}_{16}$	28	4.55	0.25
$\text{Li}_{15.5}\text{Mg}_{0.25}\text{Ge}_4\text{O}_{16}$	28	3.20	0.27

7

8

1 **Table S3.** Calculated lattice parameters of $\text{Li}_{16-2x}\text{M}_{x/2}\text{Cd}_{x/2}\text{Ge}_4\text{O}_{16}$ (M = Zn, Mg)

2 from DFT.

Composition	cell	a (Å)	b (Å)	c (Å)	α (°)	β (°)	γ (°)	Unit cell Volume (Å ³)
$\text{Li}_{12}\text{MgCdGe}_4\text{O}_{16}$	supercell	10.62	12.69	11.15	90.22	90.99	89.89	1502.16
$\text{Li}_{14}\text{Mg}_{0.5}\text{Cd}_{0.5}\text{Ge}_4\text{O}_{16}$	supercell	10.53	12.64	11.03	89.86	89.89	90.58	1466.96
$\text{Li}_{15}\text{Mg}_{0.25}\text{Cd}_{0.25}\text{Ge}_4\text{O}_{16}$	supercell	10.95	12.60	10.50	89.90	90.43	89.83	1449.10
$\text{Li}_{12}\text{ZnCdGe}_4\text{O}_{16}$	supercell	10.65	12.67	11.14	90.23	90.92	90.03	1503.62
$\text{Li}_{14}\text{Zn}_{0.5}\text{Cd}_{0.5}\text{Ge}_4\text{O}_{16}$	supercell	10.55	12.65	11.03	89.89	89.88	90.60	1471.75
$\text{Li}_{15}\text{Zn}_{0.25}\text{Cd}_{0.25}\text{Ge}_4\text{O}_{16}$	supercell	10.96	12.61	10.50	89.90	90.36	89.86	1451.04

3

4

5 **Table S4.** The phase stability and diffusional properties of Li_{16-}

6 $2x\text{M}_{x/2}\text{Cd}_{x/2}\text{Ge}_4\text{O}_{16}$ (M = Zn, Mg).

Composition	E_{hull} (meV/atom)	$\sigma_{300\text{K}}$ (mS/cm)	E_a (eV)
$\text{Li}_{12}\text{ZnCdGe}_4\text{O}_{16}$	22	1.36	0.27
$\text{Li}_{14}\text{Zn}_{0.5}\text{Cd}_{0.5}\text{Ge}_4\text{O}_{16}$	28	2.48	0.27
$\text{Li}_{15}\text{Zn}_{0.25}\text{Cd}_{0.25}\text{Ge}_4\text{O}_{16}$	30	1.20	0.30
$\text{Li}_{12}\text{MgCdGe}_4\text{O}_{16}$	23	0.23	0.34
$\text{Li}_{14}\text{Mg}_{0.5}\text{Cd}_{0.5}\text{Ge}_4\text{O}_{16}$	28	3.70	0.25
$\text{Li}_{15}\text{Mg}_{0.25}\text{Cd}_{0.25}\text{Ge}_4\text{O}_{16}$	30	3.33	0.26

7

8

1 **Table S5.** The impact of cation (Cd and Mg) on ΔE_{site} in $\text{Li}_{14}\text{Zn}_{0.5}\text{Cd}_{0.5}\text{Ge}_4\text{O}_{16}$.

Zn_impact	E(eV)	Cd_impact	E(eV)
E site	-770.623	F site	-770.258
E' site	-769.497	F' site	-769.506
ΔE_{site}	1.126	ΔE_{site}	0.752

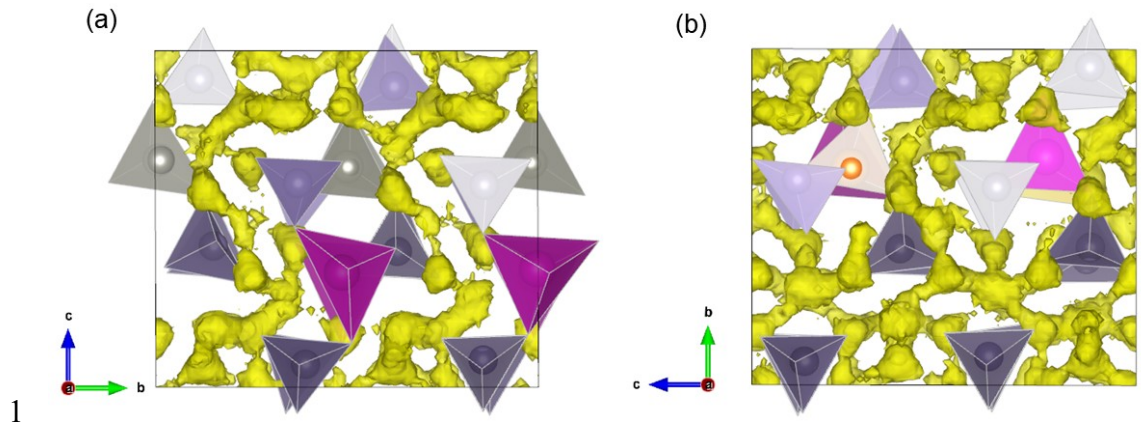
2

3 **Table S6.** The phase stability and diffusional properties of

4 $\text{Li}_{15}\text{Zn}_{0.25}\text{Mg}_{0.25}\text{Ge}_4\text{O}_{16}$ and $\text{Li}_{12}\text{MgZnGe}_4\text{O}_{16}$.

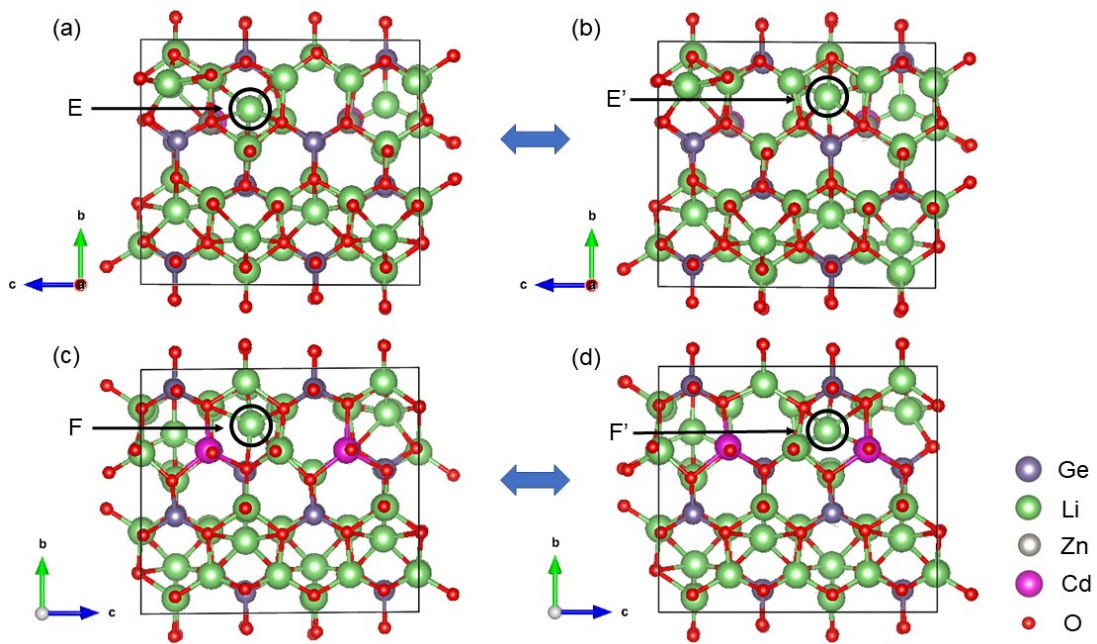
Composition	E_{hull} (meV/atom)	$\sigma_{300\text{K}}$ (mS/cm)	E_a (eV)
$\text{Li}_{15}\text{Zn}_{0.25}\text{Mg}_{0.25}\text{Ge}_4\text{O}_{16}$	27	3.00	0.26
$\text{Li}_{12}\text{MgZnGe}_4\text{O}_{16}$	16	0.09	0.37

5



1
 2 **Figure S1.** The probability densities of Li ions that was calculated by AIMD
 3 simulations at 900 K (a) in $\text{Li}_{12}\text{ZnCdGe}_4\text{O}_{16}$ and (b) in $\text{Li}_{12}\text{MgCdGe}_4\text{O}_{16}$ (yellow
 4 dots are used to represent the possible positions of lithium ions).

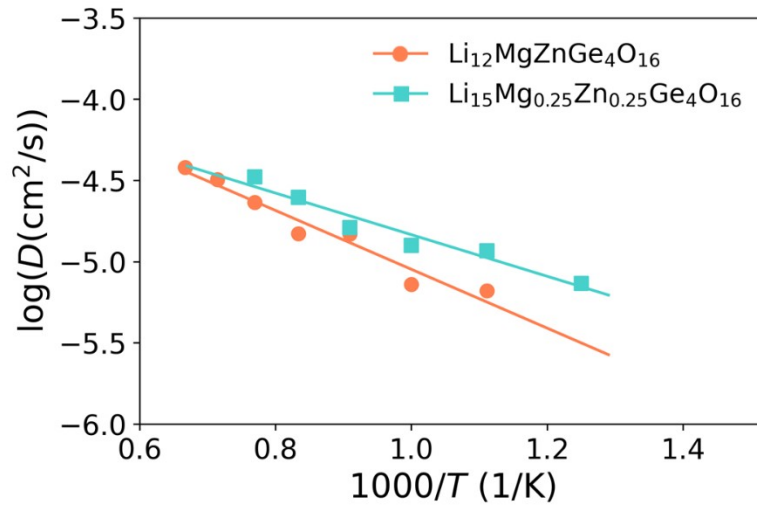
5



6

7 **Figure S2.** The comparison of Cd and Zn impacts in $\text{Li}_{14}\text{Zn}_{0.5}\text{Cd}_{0.5}\text{Ge}_4\text{O}_{16}$. E
 8 site in (a), E' site in (b), F site in (c), F' site in (d).

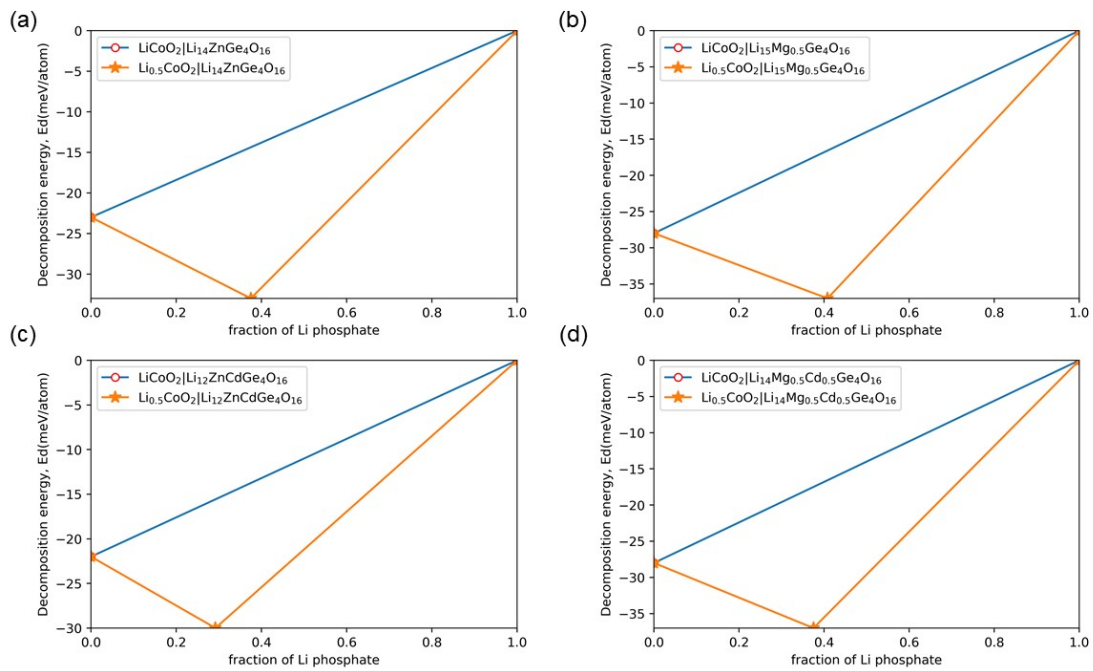
9



1

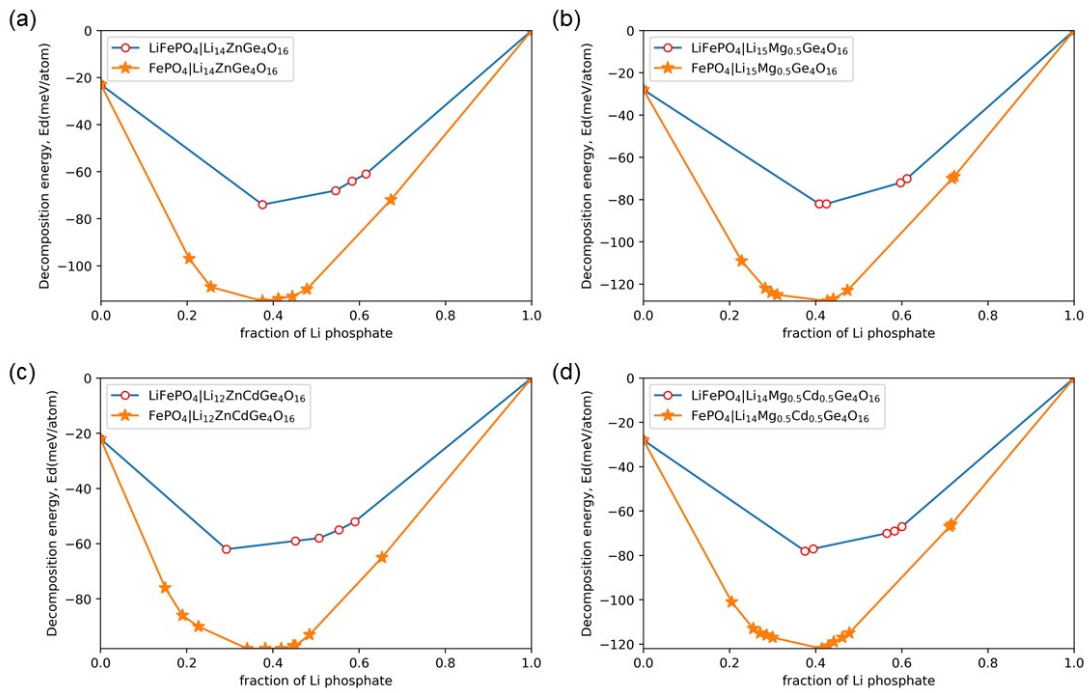
2 **Figure S3.** Arrhenius plots of Li ions diffusion in $\text{Li}_{12}\text{MgZnGe}_4\text{O}_{16}$ and
 3 $\text{Li}_{15}\text{Mg}_{0.25}\text{Zn}_{0.25}\text{Ge}_4\text{O}_{16}$ from AIMD simulation.

4



5

6 **Figure S4.** Decomposition energy of between (a) LCO and $\text{Li}_{14}\text{ZnGe}_4\text{O}_{16}$
 7 (LiCoO_2 represents discharging status, $\text{Li}_{0.5}\text{CoO}_2$ represents charging state);
 8 (b) LCO and $\text{Li}_{15}\text{Mg}_{0.5}\text{Ge}_4\text{O}_{16}$; (c) LCO and $\text{Li}_{12}\text{ZnCdGe}_4\text{O}_{16}$; (d) LCO and
 9 $\text{Li}_{14}\text{Mg}_{0.5}\text{Cd}_{0.5}\text{Ge}_4\text{O}_{16}$.

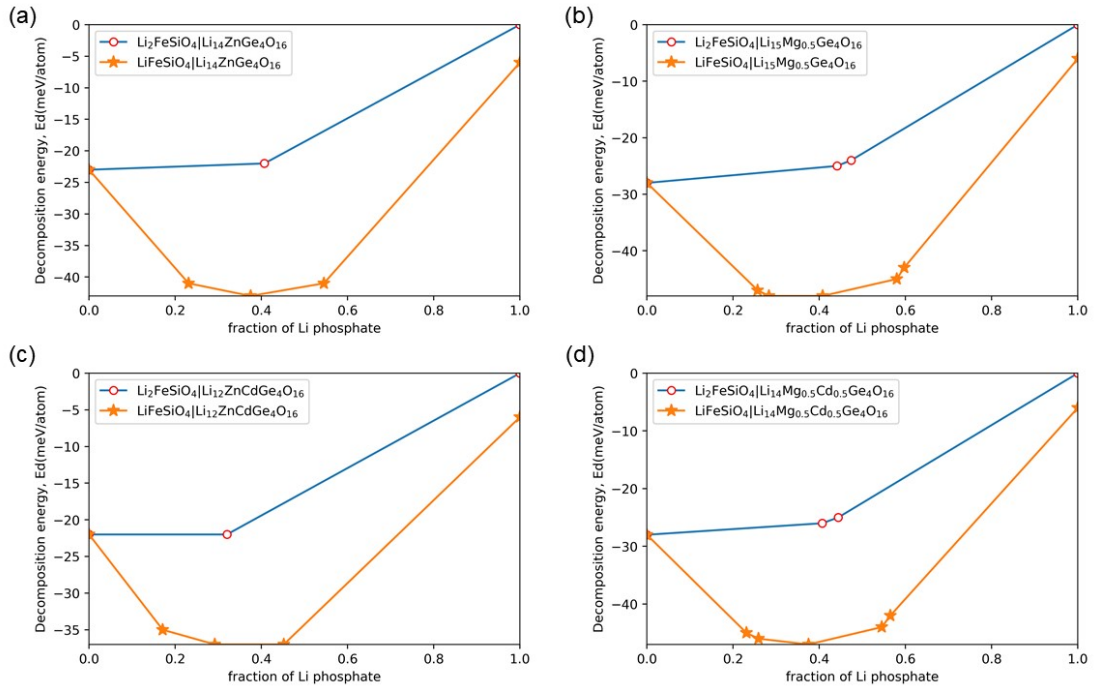


1

2 **Figure S5.** Decomposition energy of between (a) LFPO and $\text{Li}_{14}\text{ZnGe}_4\text{O}_{16}$
 3 (LiFePO_4 represents discharging status, FePO_4 represents charging state); (b)
 4 LFPO and $\text{Li}_{15}\text{Mg}_{0.5}\text{Ge}_4\text{O}_{16}$; (c) LFPO and $\text{Li}_{12}\text{ZnCdGe}_4\text{O}_{16}$; (d) LFPO and
 5 $\text{Li}_{14}\text{Mg}_{0.5}\text{Cd}_{0.5}\text{Ge}_4\text{O}_{16}$.

6

7



1

2 **Figure S6.** Decomposition energy of between (a) LFSO and $\text{Li}_{14}\text{ZnGe}_4\text{O}_{16}$

3 ($\text{Li}_2\text{FeSiO}_4$ represents discharging status, LiFeSiO_4 represents charging state);

4 (b) LFSO and $\text{Li}_{15}\text{Mg}_{0.5}\text{Ge}_4\text{O}_{16}$; (c) LFSO and $\text{Li}_{12}\text{ZnCdGe}_4\text{O}_{16}$; (d) LFSO and

5 $\text{Li}_{14}\text{Mg}_{0.5}\text{Cd}_{0.5}\text{Ge}_4\text{O}_{16}$.

6

1 Note 1:

2 In the studies of thio-LISICON type solid electrolyte, when the solid
3 solution member $x = 0.75$ $\text{Li}_{4-x}\text{Ge}_{1-x}\text{P}_x\text{S}_4$ shows the highest conductivity,
4 namely $\text{Li}_{9.75}\text{Ge}_{0.75}\text{P}_{2.25}\text{S}_{12}$.¹ Therefore, in theory the lithium-ion concentration
5 of $\text{Li}_{10}\text{GeP}_2\text{S}_{12}$ exceeds the optimal value possibly. If further improving the
6 lithium-ion conductivity of $\text{Li}_{10}\text{GeP}_2\text{S}_{12}$, according to we proposed doping
7 theory, it should be doped with cations with smaller radii. In the study of
8 $\text{Li}_{10}(\text{Ge}_{1-x}\text{M}_x)\text{P}_2\text{S}_{12}$ ($\text{M} = \text{Si}, \text{Sn}$), $\text{Li}_{10}\text{Ge}_{0.95}\text{Si}_{0.05}\text{P}_2\text{S}_{12}$ possess slightly higher
9 lithium-ion conductivity than $\text{Li}_{10}\text{GeP}_2\text{S}_{12}$ at 300 K. However, doping with
10 large-radius non-lithium cations would cause the decrease in Li-ion
11 conductivity. Interestingly, in all Sn-doped materials their lithium-ion
12 conductivity all are lower than that of $\text{Li}_{10}\text{GeP}_2\text{S}_{12}$.² Similarly, in experimental
13 studies of $\text{Li}_{10}\text{Ge}_{1-x}\text{Sn}_x\text{P}_2\text{S}_{12}$ the similar results were also observed.³
14 Furthermore, based on first-principles calculations, the order of Li-ion
15 conductivity of these materials is $\text{Li}_{10}\text{GeP}_2\text{S}_{12} > \text{Li}_{10}\text{SnP}_2\text{S}_{12}$.⁴ Therefore,
16 based on the above observations, our proposed doping strategies probably
17 also are applicable to thio-LISICON type solid electrolyte.

18

19

1 References

- 2 1 R. Kanno and M. Murayama, *J. Electrochem. Soc.*, 2001, **148**, A742.
- 3 2 Y. Kato, R. Saito, M. Sakano, A. Mitsui, M. Hirayama and R. Kanno, *J.*
4 *Power Sources*, 2014, **271**, 60-64.
- 5 3 T. Krauskopf, S. P. Culver and W. G. Zeier, *Chem. Mater.*, 2018, **30**,
6 1791-1798.
- 7 4 S. P. Ong, Y. Mo, W. D. Richards, L. Miara, H. S. Lee and G. Ceder,
8 *Energy Environ. Sci.*, 2013, **6**, 148-156.
- 9